

# Supplementary Information – Measurement-Induced Entanglement for Excitation Stored in Remote Atomic Ensembles

C. W. Chou, H. de Riedmatten, D. Felinto, S. V. Polyakov, S. J. van Enk,<sup>†</sup> and H. J. Kimble

*Norman Bridge Laboratory of Physics 12-33*

*California Institute of Technology, Pasadena, CA 91125*

<sup>†</sup>*Bell Labs, Lucent Technologies, Room 1D-428*

*600-700 Mountain Ave, Murray Hill, NJ 07974*

(Dated: November 17, 2005)

Supporting documentation is provided for our paper Ref. [1].

## I. EXPERIMENTAL DETAILS

### A. Losses and efficiencies

In order to infer the concurrence of the fields at different locations in our experimental apparatus it is important to characterize the losses in the different components of the communication channels of fields 2. Our measurements for such losses are given in the table below for the pathways starting from each of the atomic ensembles. Immediately after the ensembles, we separate the classical pulses from fields 1 and 2 in the single-photon level. This procedure is explained in detail in Refs. [2, 3]. The losses coming from this stage are due mainly to passage through paraffin coated vapor cells, which have transmission  $\alpha_{fc}$ . After the filtering process, field 2 is coupled to a polarization maintaining fiber that carries it to the detection region. The coupling efficiency is denoted by  $\alpha_c$ . In the detection region, it is important first to filter the 1.06  $\mu\text{m}$  light that propagates together with field 2, and which is used to actively lock the read interferometer when  $BS_2$  is inserted. In order to filter the 1.06  $\mu\text{m}$  light, field 2 comes out of the fiber and passes through a bulk low-pass filter that reflects 1.06  $\mu\text{m}$  light and transmits with high efficiency at 894 nm. At this stage, we also include an extra filter for 852 nm, to cut any residual light from the write process, and then field 2 is coupled again to a fiber, this time a multi-mode one. This whole process of passing through the band-pass filters and recoupling to fiber is called generally “filter for 1064 nm”, and is characterized by a transmission  $\alpha_f$ . Finally, the detector efficiencies are given by  $\alpha_{APD}$ . Note that a single number is given for the pair of detectors  $D_{2b,2c}$ , since they both have measured efficiencies of 40%.

Description	Symbol	Value for ensemble L	Value for ensemble R	Error
filter cell	$\alpha_{fc}$	0.80	0.80	0.02
fiber coupling	$\alpha_c$	0.70	0.65	0.02
1064 nm filter	$\alpha_f$	0.70	0.70	0.02
detector	$\alpha_{APD}$	0.32	0.40	0.02
Total	$\alpha$	0.13	0.15	

TABLE 1: List of efficiencies associated with photon 2 propagation and detection.

### B. Suppression of interference between the $2_L, 2_R$ fields for distinguishable detection events from the fields $1_L, 1_R$

In our experiment, entanglement is generated by quantum interference between the fields 1 emitted by the ensembles, that are combined at a beam-splitter and detected. For this interference to occur, the two fields must be indistinguishable, such that no information can be obtained about the origin of the photons. A good way to illustrate the importance of this overlap is to render the photons distinguishable, for instance by combining the two fields 1 with orthogonal polarizations. In this way, information about the origin of the detected photon is near maximal, and the degree of measurement-induced entanglement should be significantly reduced (to zero in the ideal case). The results of such a measurement are shown in Fig. 1. Fig. 1(a,b) shows the interference fringes obtained when the photons of field 1 are combined with parallel polarizations (same fringes as in Fig. 2 in Ref [1]), while in Fig. 1(c,d), the photons from field 1 are combined with orthogonal polarizations. In the latter case, the visibility drops to near zero, and there is no entanglement between the two ensembles. The residual oscillation in the conditional count rate

can be explained by the finite polarization extinction ratio in our polarization maintaining fibers. The fibers used in our experiment have a measured extinction ratio of 28 dB between their two orthogonal propagation modes. This can lead to a residual visibility of 8 %, which is compatible with the amplitude of the residual oscillation in Fig. 1(c,d).

### C. Asymmetry in the creation of the states conditioned on $D_{1a}$ and $D_{1b}$

The difference in the two sets of probabilities  $(p_{01}^{(1a)}, p_{10}^{(1a)})$  and  $(p_{01}^{(1b)}, p_{10}^{(1b)})$  results from an asymmetry in the beam splitter  $BS_1$  for detection of the write fields  $1_L, 1_R$ , with a measured ratio of transmission to reflection  $T/R = 0.85$ . Hence, in addition to the  $\pm$  sign in Eq. 1 of Ref. [1] set by detection at  $D_{1a}$  or  $D_{1b}$ , the relative amplitudes for the conditional state can also differ, resulting in different values for the concurrence. We expect the ratio  $(p_{01}^{(1a)}/p_{10}^{(1a)})(p_{01}^{(1b)}/p_{10}^{(1b)})^{-1}$  to be  $(T/R)^2 = 0.73$ , which agrees well with the measured value  $(7.51/7.38)(8.78/6.19)^{-1} = 0.72$ .

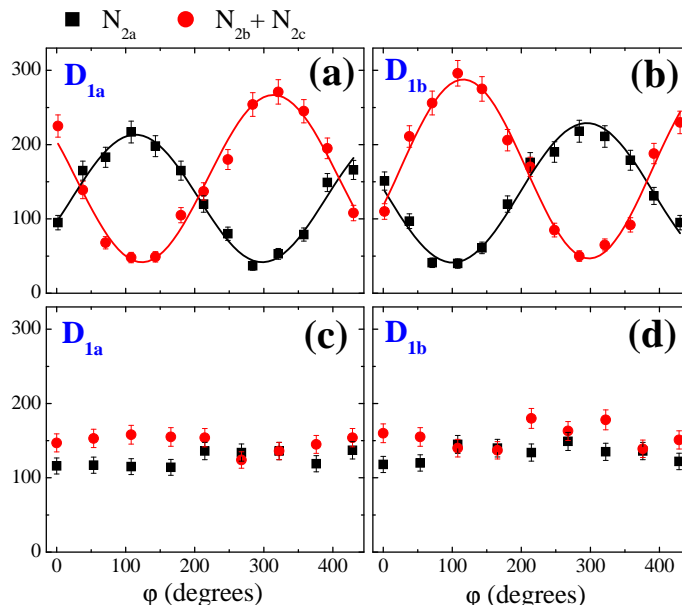


FIG. 1: Number of coincidences  $N_{2a}$  (squares) and  $N_{2b} + N_{2c}$  (circles) recorded by the respective detectors  $D_{2a,2b,2c}$  for the fields  $2_L, 2_R$  with the interferometer arrangement of Fig. 1(b) of Ref. [1] as a function of the relative phase  $\varphi$ . Frames (a) and (b) are the same as frames (a) and (b) of Fig. 2 of Ref.[1], i.e., they show the interference fringe between fields  $2_L, 2_R$  as a result of combining fields  $1_L, 1_R$  in an approximately indistinguishable fashion with parallel polarizations. Frames (c) and (d) show the results of the same measurement on fields  $2_L, 2_R$ , but now with fields  $1_L, 1_R$  combined with orthogonal polarizations. At each setting of  $\varphi$ , data are acquired for 150 s with a detection window of width 190 ns.

### D. Verification of single excitation regime

Apart from the parameter  $h_c^{(2)}$  discussed previously, another measure of the single-photon character of field 2 is given by the evaluation of the function  $\tilde{g}_{12} = \tilde{p}_{12}/(\tilde{p}_1\tilde{p}_2)$  for each ensemble separately [2, 3], where  $\tilde{p}_{12}$  is the joint probability of detecting a photon in field 1 and another in field 2, and  $\tilde{p}_i$  is the probability of detecting a single photon in field  $i$ . For the situation of our measurement, we obtained  $\tilde{g}_{12}$  values of about 9 and 11 for ensembles  $R$  and  $L$ , respectively, which is then an indication of the single-photon character of field 2 emitted by both ensembles separately, conditioned on a write detection event, as discussed in [3].

### E. Phase stabilization

The  $\approx 12$  m path lengths for the two interferometers formed by  $(BS_w, BS_1)$  and by  $(BS_R, BS_2)$  shown in Figures 1(a) and 1(b) of Ref.[1], respectively, are held constant by injecting an iodine stabilized Nd:YAG laser into the fiber

beam splitters  $BS_w, BS_R$  for the write and read beams. The fields at  $1.064 \mu\text{m}$  emerging from beam splitters  $BS_1, BS_2$  are directed to separate sets of detectors (not shown in the figure), whose outputs are used to stabilize the relative path lengths of the respective Mach-Zehnder interferometers by feedback to piezoelectric transducers on which are mounted mirrors in the paths of the write and read beams in the  $L$  arms of the respective interferometers. Since the write and read beams are combined together before being focused into the ensembles, the interferometers share a common free space path when they cross the atoms. In order to control them independently and minimize crosstalk, the two interferometers are addressed alternately at a rate of 400 kHz.

## F. Normalization and detector configuration

The role of the three detectors in our experiment is as a second check on the order of magnitude of the two-photon events. Our main checks were discussed in Ref.[1] and in section ID of this Supplementary Information. It is interesting to obtain directly  $p_{02}$  and have an idea of its effect on  $p_{01}$ . For our measurement, we obtained, with  $D_{2b}$  and  $D_{2c}$ ,  $p_{02} = (2.2 \pm 0.4) \times 10^{-5}$  conditioned on detector  $D_{1a}$ , and  $p_{02} = (2.4 \pm 0.4) \times 10^{-5}$  conditioned on detector  $D_{1b}$ . These values are obtained at the location of the detectors, assuming a unit quantum efficiency and without any corrections for background or dark counts. Note that these values are so small that if taken into account, the correction for  $p_{10}$  and  $p_{01}$  would be negligible and within the quoted uncertainties. In order to simplify our analysis and inversion algorithm, we consider the three detectors as an effective set of two detectors. This is done by simply adding the coincidence events between  $D_{2b}$  and  $D_{2c}$  to the sum  $N_{2b} + N_{2c}$ , in the same way that would result from the use of a non-number-resolving detector. In this case, the measured normalization constant  $\tilde{P}$  is equal to one, since every measured event contributes to one of the elements of the restricted density matrix. If we had used more detectors, the discrepancy of  $\tilde{P}$  from unity would be on the order of  $p_{02}$  and again small compared to the experiment accuracy and statistical uncertainties.

## II. THEORY

### A. Entanglement

For convenience of description we assume the two atomic ensembles  $L$  and  $R$  to be in the hands of Alice and Bob, respectively. The state of the two ensembles conditioned on a click of one of the two detectors  $D_{1a}$  or  $D_{1b}$  (see Figure 1b of Ref.[1]) is mapped onto a state of multiple field modes belonging to Alice and multiple modes belonging to Bob. Because the mapping involves only *local* operations by Alice and Bob, the entanglement (in particular, the entanglement of formation) between their systems cannot increase on average [4]. Hence the entanglement found between Alice's and Bob's field modes is a lower bound on the entanglement between the atomic ensembles. We will use this type of reasoning several times here: certain experimental procedures can be exactly mimicked by imagining Alice and Bob performing LOCC (local operations and classical communication): those operations cannot increase the entanglement we find. We also sometimes set a lower bound on the entanglement analytically, using quantities that are more straightforward to measure in the laboratory. That way, we can unambiguously determine the presence of entanglement between the two ensembles, even if we might underestimate its actual magnitude.

On each side there is one main mode (a traveling mode) into which photons are emitted predominantly [5]. Those modes we denote by  $2_L$  and  $2_R$ . Other modes may be populated with very small probability, but in the analysis we assume all detector clicks arise from modes  $2_L$  and  $2_R$ . In the experiment this reduction from multiple to single modes is mainly accomplished by the use of single mode fibers, which filter out different spatial modes. This is a procedure that can be exactly mimicked by Alice and Bob performing that same spatial filtering on their local modes and hence can only decrease the actual entanglement.

We also assume that never more than 2 photons populate each mode. This is an excellent approximation on its own (and is supported by our measurements), but more importantly, this assumption corresponds to lower bounding the entanglement, as detailed below.

We furthermore assume that all off-diagonal elements of the density matrix between states with different numbers of photons vanish. This is a valid assumption when one takes into account that phase can only be defined relative to a reference laser beam shared by Alice and Bob. Tracing out that laser field sets the off-diagonal elements to zero. Indeed, the experiment makes no use of knowledge of the phases of the various lasers used. Moreover, this can only underestimate the entanglement, since tracing out the laser modes can be exactly mimicked by Alice and Bob performing local operations that makes all those off-diagonal elements zero. Namely, they could each apply a random phase shift to their modes, such that the phase difference is fixed (this requires classical but not quantum

communication), and subsequently ignore the information about the individual phase shifts. The phase difference is equal to the phase  $\varphi$  introduced in Ref.[1].

This then leaves us with a density matrix of the form

$$\rho_{2L,2R} = \begin{pmatrix} p_{00} & 0 & 0 & 0 & 0 & 0 \\ 0 & p_{01} & d & 0 & 0 & 0 \\ 0 & d^* & p_{10} & 0 & 0 & 0 \\ 0 & 0 & 0 & p_{11} & e & f \\ 0 & 0 & 0 & e^* & p_{02} & g \\ 0 & 0 & 0 & f^* & g^* & p_{20} \end{pmatrix}.$$

We can bound the concurrence of this state by

$$C(\rho_{A,B}) \geq \tilde{P}C(\tilde{\rho}_{2L,2R}) \quad (1)$$

where

$$\tilde{P} = p_{00} + p_{01} + p_{10} + p_{11} \quad (2)$$

$$\tilde{\rho}_{2L,2R} = \frac{1}{\tilde{P}} \begin{pmatrix} p_{00} & 0 & 0 & 0 \\ 0 & p_{01} & d & 0 \\ 0 & d^* & p_{10} & 0 \\ 0 & 0 & 0 & p_{11} \end{pmatrix}. \quad (3)$$

One obtains this bound by considering the effects of two local operations by Alice and Bob consisting of measuring whether each mode has more than 1 photon or not and communicating this result one to the other. We treat this step explicitly and separately from the very similar step mentioned above [where cases with more than two photons are filtered out], in order to remind ourselves we do have to keep track of the total probability to find more than 1 photon in one of the modes,  $1 - \tilde{P}$ . Also, we note explicitly this step does not correspond to any procedure in our experiment, but is just an analytic tool to bound the entanglement and express it in terms of quantities that can be easily determined without too large uncertainty (unlike higher-order matrix elements such as  $p_{12}$ , etc).

### 1. Detection window

In Fig. 3 of Ref[1], we show results for a smaller detection window that give a higher estimation for the amount of entanglement between the fields. The use of a smaller detection window can also be understood as a reduction from multiple to single modes by filtering out different temporal modes. This is a procedure that can be exactly mimicked by Alice and Bob performing that same temporal filtering on their local modes and hence can only decrease the actual entanglement (note though, that the *estimate* of entanglement can be increased by this procedure, even though the actual entanglement decreases. The estimated value just gets closer to the actual value than when not filtering out extraneous modes).

For the possibly remaining multiple modes in the smaller time window, we may suppose Alice and Bob each apply the following fictitious transformation

$$|n_1\rangle|n_2\rangle \dots \rightarrow \left| \sum_i n_i \right\rangle |n_1, n_2, \dots\rangle_M$$

to their local modes. This transformation collects all photons in one mode (the first ket), and keeps track of where they came from in a separate system  $M$  (for “memory”), such that the transformation is unitary. This transformation, therefore, leaves the entanglement between Alice’s and Bob’s mode unchanged. Our detectors not being able to distinguish different modes within the same time window then boils down to tracing out the memory system, which can only decrease the entanglement.

### 2. Single particle entanglement

One sometimes sees objections to calling entangled a state of the form

$$|\Psi\rangle_{AB} = |0\rangle_A|1\rangle_B \pm |1\rangle_A|0\rangle_B \quad (4)$$

where  $A$  and  $B$  are two spatially separated modes of light fields and  $|n\rangle$ ,  $n = \{0, 1\}$  is a Fock state containing  $n$  photons. One objection is that there is only one photon present, and one might think one needs at least two photons (or particles) to have entanglement. However, the state (4) can be converted into an entangled state with 2 particles by *local* operations, thus demonstrating entanglement in the original state [6]. A second objection [7] applies to the case where the phase between  $|0\rangle|1\rangle$  and  $|1\rangle|0\rangle$  is not defined, such as when there is no phase reference present. Indeed, in that case one would not have a state of the form (4) but a mixed unentangled state instead. In our experiment, however, the phase is well-defined and hence we conclude, again, that the state (4) is genuinely entangled. The issue is discussed in more detail in [6].

## B. Measurements

All measurements are performed using Geiger-mode avalanche photodiodes (APDs). We assume there are only two outcomes of a photodetection measurement, corresponding to no click or some nonzero number of clicks (indeed, that is the only information used in the experiment). Thus, if the incoming mode  $2_L$  is described by an annihilation operator  $a$  then the photodetector performs a POVM of the form

$$\begin{aligned}\Pi_0 &= \sum_{n \geq 0} (-1)^n \frac{a^{\dagger n} a^n}{n!} \\ \Pi_1 &= I_A - \Pi_0,\end{aligned}\tag{5}$$

with  $I_A$  the identity on  $2_L$ . The corresponding probabilities are denoted by  $p_0$  and  $p_1$ ,

$$p_k = \text{Tr} \rho_{2_L} \Pi_k,\tag{6}$$

if  $\rho_{2_L}$  is the state of mode  $2_L$ . To deduce higher-order probabilities with  $k \geq 2$ , beam splitters can be employed to divide and direct the mode  $a$  to multiple detectors.

Joint probabilities for measurements on the two modes  $2_L$  and  $2_R$  can be determined in a similar way if we introduce the annihilation operator  $b$  for mode  $2_R$  and the corresponding operators  $\Pi_n^{A,B}$  for  $n = 0, 1$  for the two modes. The operators  $\Pi_0$  and  $\Pi_1$  above were written in normal order. Similarly, joint measurement probabilities can be written as

$$P_{mn} = \text{Tr} \tilde{\rho}_{2_L, 2_R} : \Pi_m^A \otimes \Pi_n^B :, \tag{7}$$

where all annihilation operators  $a$  and  $b$  are written to the right of all creation operators  $a^\dagger$  and  $b^\dagger$ . For example, this allows one to include easily the effects of finite efficiencies of detectors: If  $\eta$  is the efficiency of a detector and  $a$  the annihilation operator for the mode impinging on the detector, we may replace  $a \rightarrow \sqrt{\eta}a + \sqrt{1-\eta}v$  where  $v$  acts on an auxiliary mode that is assumed to be in the vacuum state. Terms with nonzero powers of  $v$  then do not contribute to counting rates provided we evaluate these by using a normally-ordered expression. In that case, we can ignore  $v$  and just replace  $a \rightarrow \sqrt{\eta}a$ . The same replacement can be used to take into account losses during propagation.

The most straightforward way to determine  $\tilde{\rho}_{2_L, 2_R}$  consists of two stages. The first stage determines the diagonal elements, the second the off-diagonal elements: From the measured frequencies of joint detection events we obtain estimates for the corresponding probabilities for those joint events in terms of the underlying density matrix elements. Inverting these expressions gives estimates on the elements of the density matrix.

### 1. Diagonal elements

Conditioned upon detection of an event at either detector  $D_{1a}$  or  $D_{1b}$ , the diagonal elements of  $\tilde{\rho}_{2_L, 2_R}$  were measured by the setup described in Figure 1(b) of Ref.[1]. Photons in mode  $2_L$  are detected by a photodetector  $D_{2a}$  but mode  $2_R$  is split on a 50/50 (approximately) beamsplitter and photons in the two resulting modes are counted by photodetectors  $D_{2b}$  and  $D_{2c}$ . Starting with mode operators  $a$  and  $b$  for modes  $2_L$  and  $2_R$ , there are several transformations affecting  $a$  and  $b$ . Denoting by  $a_1$  the mode operator detected by detector  $D_{2a}$ , and by  $b_1$  and  $b_2$  those detected by  $D_{2b}$  and  $D_{2c}$ , the transformations are simply

$$\begin{aligned}a_1 &= \sqrt{\eta_L \eta_1} a \\ b_2 &= \sqrt{\eta_R \eta_2} b / \sqrt{2} \\ b_3 &= \sqrt{\eta_R \eta_3} b / \sqrt{2}\end{aligned}\tag{8}$$

with  $\eta_{L,R}$  indicating the total efficiency of propagating to the detectors, and  $\eta_{1,2,3}$  the detector efficiencies of detectors  $D_{2a}, D_{2b}, D_{2c}$ . One then obtains expressions for the expected joint count probabilities  $p_{klm}$  with  $k, l, m = 0, 1$  by substituting (8) into (5) and (7). When acting on  $\tilde{\rho}_{2L,2R}$  the operators  $a$  and  $b$  are understood to be  $a \otimes I_B$  and  $I_A \otimes b$ .

In the end, we only consider the total number of counts in detectors  $D_{2a}$  and  $D_{2b}, D_{2c}$  together, leading to joint probabilities  $Q_{mn}$  with  $m = 0, 1$  and  $n = 0, 1, 2$ ,

$$Q_{mn} = \sum_m \sum_{s+t=n} P_{mst}. \quad (9)$$

Again, for these measurements as well as those in the next section, the detection events at  $D_{2a}$  and  $D_{2b}, D_{2c}$  are conditioned upon an event at either  $D_{1a}$  or  $D_{1b}$ . This gives expressions for the expected detection probabilities  $Q_{mn}$  as functions of the diagonal elements  $p_{mn}$  of the density matrix: conversely, given the experimentally determined  $Q_{mn}$  we invert the expressions to obtain estimates for  $p_{mn}$ .

## 2. Off-diagonal elements

The off-diagonal elements are measured by including two extra elements: one is a phase shifter in one of the modes, say mode  $2_L$ , thus replacing  $a \rightarrow \exp(i\varphi)a$ . This phase is varied to produce the interference pattern (“fringes”) of Figure 2. Second is an extra 50/50 beamsplitter after the phase shifter [ $BS_2$  in Fig. 1(b)]. One again easily arrives at simple expressions for the operators  $a_1$  and  $b_1, b_2$  detected in terms of  $a$  and  $b$ , similar to that of (8). Just as before, one then obtains expressions for the expected joint count probabilities  $p_{klm}$  with  $k, l, m = 0, 1$  by substituting these expressions for  $a_1, b_1, b_2$  into (5) and (7). We thus find the joint detection probabilities  $Q_{mn}^f$  for the “fringes” as a function of  $d$  and the diagonal elements of  $\tilde{\rho}_{2L,2R}$ . Since we already obtained the diagonal elements in the previous step, we then find an estimate of the off-diagonal element  $d$  from the visibility of the fringes.

Note that we have also carried out measurements with detector  $D_{2a}$  replaced by a beam splitter and a pair of APDs, as for detectors  $D_{2b}, D_{2c}$ . In this way, we confirm explicitly that higher order events with  $k \geq 2$  at  $D_{2a}$  have a negligible impact on our estimates of fringe visibility and of the probabilities  $p_{00}, p_{10}, p_{01}, p_{11}$  that enter into the determination of the concurrence  $C$ , in agreement with the independent assessment from  $D_{2b}, D_{2c}$ .

In addition to the above analysis we also performed a maximum likelihood analysis of the density matrix. Given the actually detected photon statistics for both measurements of diagonal and off-diagonal elements *together* one can, for each possible candidate density matrix  $\rho_{2L,2R}$ , calculate the probability that the actually obtained measurement outcomes occur. Maximizing that probability over all possible density matrices gives the most likely density matrix. This estimate has been used as an additional check on the inferred values quoted in the main text and their errors.

- 
- [1] Chou C. W., de Riedmatten H., Felinto D., Polyakov S. V. , van Enk S. J., and Kimble H. J., *Nature*, (2005).
  - [2] Kuzmich, A., Bowen, W.P., Boozer, A.D., Boca, A., Chou, C.W., Duan, L.-M., & Kimble, H.J., Generation of nonclassical photon pairs for scalable quantum communication with atomic ensembles. *Nature* **423**, 731-734 (2003).
  - [3] Chou, C.W., Polyakov, S.V., Kuzmich, A., & Kimble, H.J., Single-photon generation from stored excitation in an atomic ensemble. *Phys. Rev. Lett.* **92**, 213601 (2004).
  - [4] Bennett C.H., DiVincenzo D.P., Smolin J.A., and Wootters W. , Mixed state entanglement and quantum error correction, *Phys. Rev. A* **54**, 3824 (1996).
  - [5] Duan, L.-M., Lukin, M., Cirac, J. I. & Zoller, P., Long-distance quantum communication with atomic ensembles and linear optics. *Nature* **414**, 413-418 (2001).
  - [6] van Enk, S.J., Single particle entanglement, *Phys.Rev.A* 2005 (in press), quant-ph/0507189
  - [7] Wiseman, H. M. and Vaccaro, J. A., Entanglement of Indistinguishable Particles Shared between Two Parties, *Phys. Rev. Lett.* **91**, 097902 (2003)